CARBON DIOXIDE CAPTURE FROM FLUE GAS USING DRY REGENERABLE SORBENTS

QUARTERLY TECHNICAL PROGRESS REPORT

Reporting Period: April 1, 2001 to June 30, 2001

by
David A. Green
Brian S. Turk
Raghubir P. Gupta
Alejandro Lopez-Ortiz
Douglas P. Harrison*
Ya Liang*

DOE Cooperative Agreement No.: DE-FC26-00NT40923

Submitted by:

Research Triangle Institute
Post Office Box 12194
Research Triangle Park, NC 27709-2194

*Louisiana State University
Department of Chemical Engineering
Baton Rouge, LA 70803

July 2001

DISCLAIMER

ABSTRACT

Sodium based sorbents including sodium carbonate may be used to capture carbon dioxide from flue gas. A relatively concentrated carbon dioxide stream may be recoverable for sequestration when the sorbent is regenerated. Electrobalance tests indicated that sodium carbonate monohydrate was formed in a mixture of helium and water vapor at temperatures below 65°C. Additional compounds may also form, but this could not be confirmed. In the presence of carbon dioxide and water vapor, both the initial reaction rate of sodium carbonate with carbon dioxide and water and the sorbent capacity decreased with increasing temperature, consistent with the results from the previous quarter. Increasing the carbon dioxide concentration at constant temperature and water vapor concentration produced a measurable increase in rate, as did increasing the water vapor concentration at constant carbon dioxide concentration and temperature. Runs conducted with a flatter TGA pan resulted in a higher initial reaction rate, presumably due to improved gas-solid contact, but after a short time, there was no significant difference in the rates measured with the different pans. Analyses of kinetic data suggest that the surface of the sodium carbonate particles may be much hotter than the bulk gas due to the highly exothermic reaction with carbon dioxide and water, and that the rate of heat removal from the particle may control the reaction rate. A material and energy balance was developed for a cyclic carbonation/calcination process which captures about 26 percent of the carbon dioxide present in flue gas available at 250°C.

TABLE OF CONTENTS

Page

LIST OF FIGURES

LIST OF TABLES

Page

1.0 EXECUTIVE SUMMARY

The objective of this project is to develop a simple, inexpensive process to separate CO_2 as an essentially pure stream from a fossil fuel combustion system using a regenerable, sodium-based sorbent. The sorbent being used in this project is sodium carbonate which is converted to sodium bicarbonate, "baking soda" through reaction with carbon dioxide and water vapor. Sodium bicarbonate is regenerated to sodium carbonate when heated.

Louisiana State University (LSU) conducted thermogravimetric testing of sodium based sorbents to determine the effect of temperature, carbon dioxide concentration, water vapor concentration, pan size, and reactant gas flow rate. Sodium carbonate monohydrate was formed, in accordance with thermodynamic predictions, in a humidified helium atmosphere. Other compounds may also form at conditions of interest.

Both the concentration of carbon dioxide and the concentration of water vapor were found to affect the rate of reaction with sodium carbonate, which is inconsistent with a previous model based on data from the patent literature.

Research Triangle Institute (RTI) analyzed the kinetic data obtained by LSU which was reported in the report for the preceding quarter. Based on these calculations, the rate of reaction may be limited by the rate of heat removal from the sorbent particles. Because the reaction between sodium carbonate and carbon dioxide and water is highly exothermic, the particle surface where the reaction occurs may be much hotter than the bulk gas temperature. Based on data from two earlier runs, the activation energy for the carbonation reaction is approximately 7,405 cal/gmol.

2.0 INTRODUCTION

Fossil fuels used for power generation, transportation, and by industry are the primary source of anthropogenic CO_2 emissions to the atmosphere. Much of the CO_2 emission reduction effort will focus on large point sources, with fossil fuel fired power plants being a prime target. The CO_2 content of power plant flue gas varies from 4% to 9% (vol), depending on the type of fossil fuel used and on operating conditions. Although new power generation concepts that may result in CO_2 control with minimal economic penalty are under development, these concepts are not generally applicable to the large number of existing power plants.

This study is based on the use of a dry, regenerable sodium-based sorbent to remove CO_2 from flue gases. Sorbent regeneration produces a gas stream containing only CO_2 and H_2O. The H_2O may be separated by condensation to produce a pure CO_2 stream for subsequent use or sequestration. The relevant reactions based upon the use of sodium bicarbonate as the sorbent precursor are:

$$2NaHCO_3(s) \leftrightarrow Na_2CO_3(s) + CO_2(g) + H_2O(g) \quad (1)$$

CO_2 removal is accomplished via the reverse of reaction (1) while the forward step is used for sorbent regeneration and CO_2 release.

This report describes activities conducted between April 1, 2001 and June 30, 2001 by Research Triangle Institute (RTI) and subcontractors Louisiana State University (LSU) and Church and Dwight (C&D). Activities conducted this quarter include electrobalance (thermogravimetric analysis [TGA]) studies at LSU, sorbent characterization at RTI, and kinetic rate investigations, thermodynamic analyses and process simulations at RTI.

3.0 EXPERIMENTAL

3.1 Electrobalance (Thermogravimetric Analysis) Testing at LSU

Twenty experimental runs using the electrobalance reactor were completed during this quarter. One test used SBC grade 1 $NaHCO_3$, two used trona T-50, and 17 of the runs used SBC grade 3 $NaHCO_3$. The properties of these materials were described in previous quarterly reports (Green et al., 2001a; Green et al., 2001b). The three runs using SBC grade 1 and trona T-50 were repeats of runs completed during the previous quarter that gave questionable results, while the 17 runs using SBC grade 3 $NaHCO_3$ examined the effects of carbonation gas composition, temperature, and volumetric flow rate, as well as the effect of the shape of the solid sample pan. Reaction conditions for all tests completed during this quarter are summarized in Table 1.

3.2 Fluidization Testing at RTI

RTI conducted additional fluidization tests to determine pressure drops as a function of gas velocity. Tests were conducted on dried-in-place SBC grade 5 and calcined SBC grade 5, using the same apparatus described in the previous quarterly report. It had been observed in preliminary tests that the pressure drops were erratic until the sorbent materials had been dried by the fluidizing gases, thus the procedure for testing the fresh material included overnight exposure to dry flowing nitrogen in the fluidization apparatus. Duplicate tests were conducted on SBC 5 that had been calcined at 125°C for approximately 16 hours in an external furnace.

Table 1. Reaction Conditions Used in Electrobalance Tests Completed This Quarter.

Run No.	Sorbent	Initial Weight (mg)	Temp., (°C)	Carbonation Conditions				
				Gas Composition			Flow	Pan*
				CO_2	H_2O	He	(sccm)	
15	SBC 1	72.5	70	8	16	76	300	Q
16	T-50	75	80	8	16	76	300	Q
18	SBC 3	73.8	80	8	16	76	300	Q
19	SBC 3	74.7	50	0	10	90	300	Q
20	SBC 3	77	60	0	10	90	300	Q
21	SBC 3	79	70	0	10	90	300	Q
22	SBC 3	75.2	70	8	10	82	300	Q
23	SBC 3	73.3	80	8	10	82	300	Q
24	SBC 3	75.7	65	0	11	89	300	Q
25	SBC 3	75.4	65	0	10	90	300	Q
26	SBC 3	76.8	70	0	16	84	300	Q
27	SBC 3	74.5	66-67	8	16	76	600	Q
28	SBC 3	74	70	5	16	79	300	Q
29	SBC 3	75.8	80	5	16	79	300	Q
30	SBC 3	74.6	65	0	16	84	300	Q
31	SBC 3	73.5	70	5	16	79	300	F
32	SBC 3	30	70	5	16	79	300	F
33	SBC 3	74.6	60	5	16	79	300	Q
34	SBC 3	74.4	73	8	16	76	600	Q
35	SBC 3	73	71	8	16	76	900	Q

*Q=quartz cup; F=flat aluminum pan.

3.3 Additional Material Characterization Tests at RTI

Repeat BET surface area, and bulk density determinations were conducted on fresh and calcined SBC grade 5 material to confirm earlier results.

4.0 RESULTS AND DISCUSSION

4.1 Electrobalance (TGA) Testing at LSU

4.1.1 Results From Repeat Tests

Runs 15, 16, and 17 from Table 1 represented repeats of early runs in the experimental program that produced questionable results. The repeat results helped to confirm the fact that both the initial reaction rate and achievable sorbent capacity decreased with increasing temperature.

4.1.2 Reaction Products in Addition to Sodium Bicarbonate

The direct formation of hydrate via the reaction

$$Na_2CO_3(s) + H_2O(g) \rightarrow Na_2CO_3 \bullet H_2O(s) \quad (2)$$

is thermodynamically possible at reaction conditions of interest. The occurrence of simultaneous gas-solid reactions makes the quantitative interpretation of electrobalance results impossible. Hence, a number of runs using a H_2O/He atmosphere (no CO_2) were carried out to study hydrate formation.

Figure 1 shows the smoothed dimensionless weight versus time results for a series of runs using a gas composition of 10% H_2O and balance He at temperatures between 50°C and 70°C. The increases in weight at 50°C and 60°C are indicative of hydrate formation, while the constant weight at 65°C and 70°C show that no hydrate is formed at these temperatures. The horizontal line at dimensionless weight of 0.63 corresponds to the theoretical value corresponding to complete calcination; all initial values were quite close to the theoretical. The wavy nature of the curve at 60°C is attributed to the data smoothing procedure.

Complete conversion of Na_2CO_3 to $Na_2CO_3 \bullet H_2O$ corresponds to a final dimensionless weight of 0.74, which is quite close to the final experimental value at 50°C. Thermodynamic calculations using HSC Chemistry show that 59°C is the maximum temperature at which hydrate formation is possible in this gas composition. Thus the experimental results and thermodynamic calculations are in reasonable, but not perfect, agreement.

The H_2O content was increased to 16% (no CO_2) and dimensionless weight versus time results are shown in Figure 2. A small amount of hydrate was formed at 65°C but no hydrate was formed at 70°C. This result is also consistent with HSC Chemistry calculations that show 66°C to be the maximum temperature for hydrate formation at this higher H_2O concentration. The predicted H_2O concentration required for hydrate formation at 70°C is 19.5%, which is above the maximum value of interest.

Additional compounds such as $Na_2CO_3 \bullet NaHCO_3 \bullet 2H_2O$ and $Na_2CO_3 \bullet 3NaHCO_3$ may also be formed from Na_2CO_3 at appropriate temperatures and pressures in gases containing both CO_2 and H_2O. Stoichiometric equations for the formation of these materials are

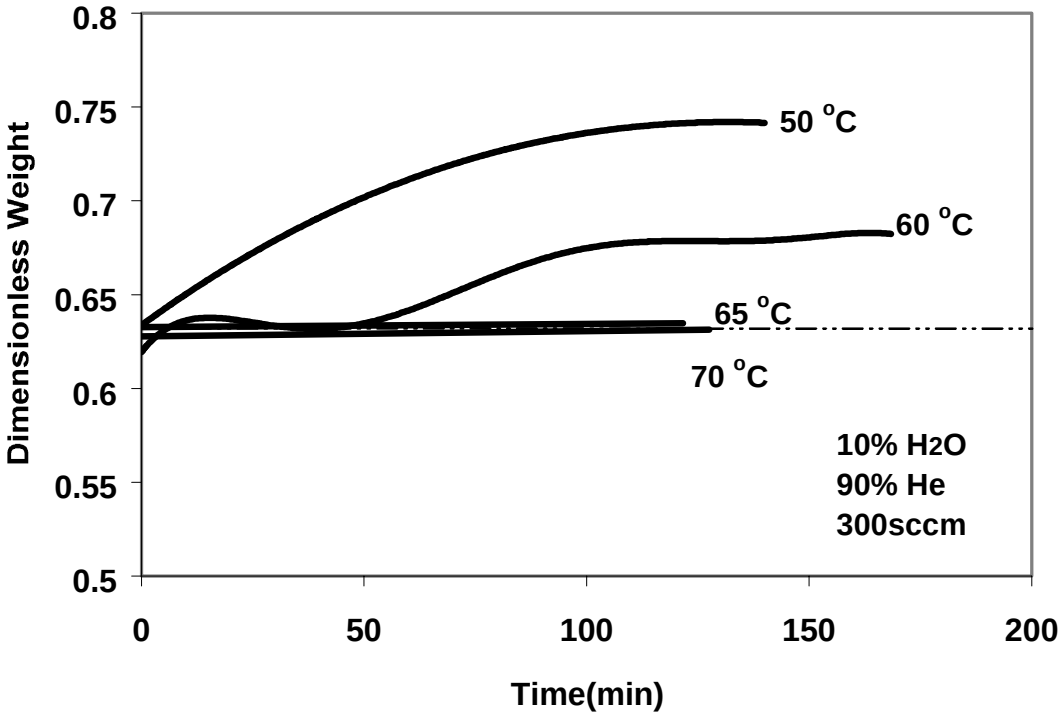

Figure 1. Hydrate formation in the presence of 10% H_2O

$$3Na_2CO_3(s) + 5H_2O(g) + CO_2(g) \rightarrow 2[Na_2CO_3 \bullet NaHCO_3 \bullet 2H_2O(s)] \quad (3)$$

$$2.5Na_2CO_3(s) + 1.5H_2O(g) + 1.5CO_2(g) \rightarrow Na_2CO_3 \bullet 3NaHCO_3(s) \quad (4)$$

However, their formation cannot be confirmed or eliminated using the electrobalance reactor. HSC Chemistry thermodynamic calculations were made using gas compositions of experimental interest and the maximum temperatures for formation of these two compounds are summarized in Table 2.

While both Na_2CO_3•$NaHCO_3$•$2H_2O$ and Na_2CO_3•$3NaHCO_3$ formation result in the removal of CO_2 from the gas phase, the sorbent efficiency, expressed as mass CO_2 removed per mass of original Na_2CO_3, is lower than when the product is $NaHCO_3$.

4.1.3 The Effect of Temperature

Results reported in the previous quarter showed that both the initial reaction rate and the achievable sorbent capacity decreased with increasing temperature when exposed to carbonation gas containing 8% CO_2, 16% H_2O, and balance He. These results were confirmed during the present quarter using different gas compositions as illustrated in Figures 3 and 4.

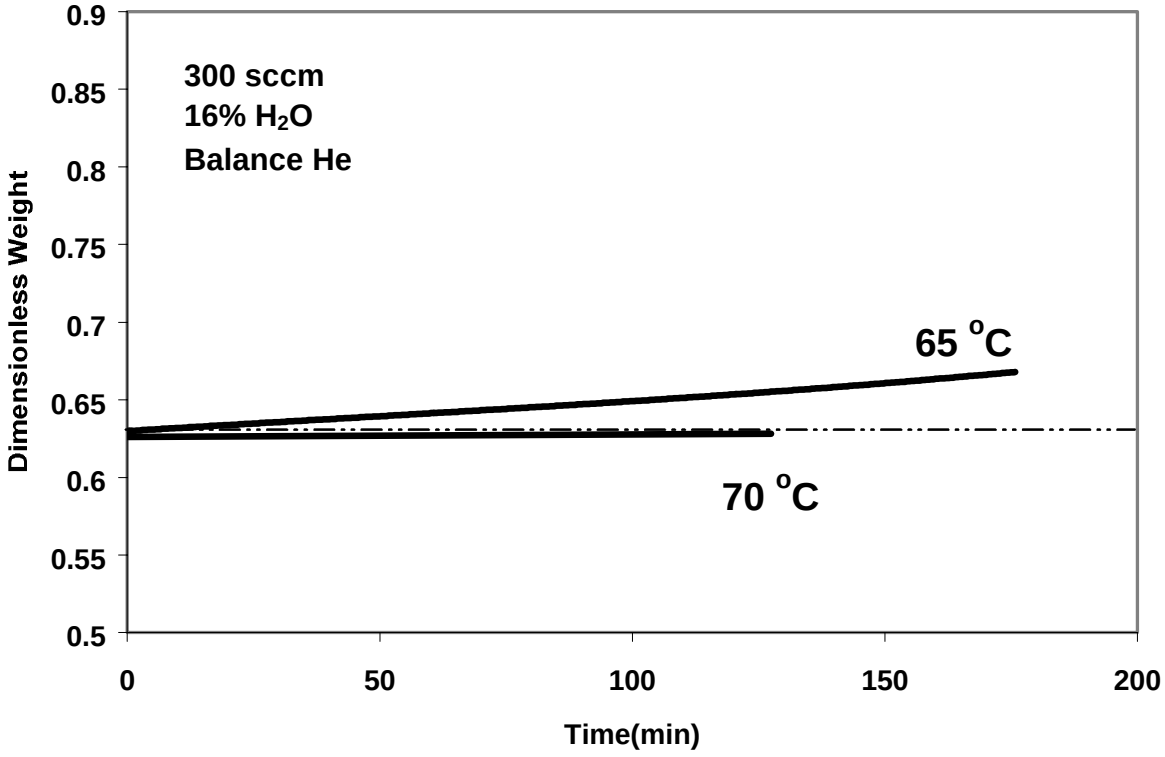

Figure 2. Hydrate formation in presence of 16% H_2O

Figure 3 shows dimensionless weight versus time results using a carbonation gas containing 5% CO_2, 16% H_2O, balance He at temperatures of 60°C, 70°C, and 80°C. Reaction occurred at both 60°C and 70°C but there was no reaction at 80°C. HSC Chemistry predicts that a minimum CO_2 pressure of 0.026 atm is required for the formation of $NaHCO_3$ at 80°C and H_2O pressure of 0.16 atm. Thus, while $NaHCO_3$ formation was thermodynamically possible at 80°C, none was formed. Table 2 shows that $Na_2CO_3 \bullet 3NaHCO_3$ formation was possible at 80°C, but that the formation of $Na_2CO_3 \bullet NaHCO_3 \bullet 2H_2O$ was not thermodynamically feasible.

Table 2. Maximum Temperatures for Formation of Byproducts as a Function of Gas Composition at 1 atm

Gas Composition (mol%)		Maximum Temperature (°C) for Formation of	
% CO_2	% H_2O	$Na_2CO_3 \bullet NaHCO_3 \bullet 2H_2O$	$Na_2CO_3 \bullet 3NaHCO_3$
8	16	74	85
8	10	67	81
5	16	72	81
5	10	66	77

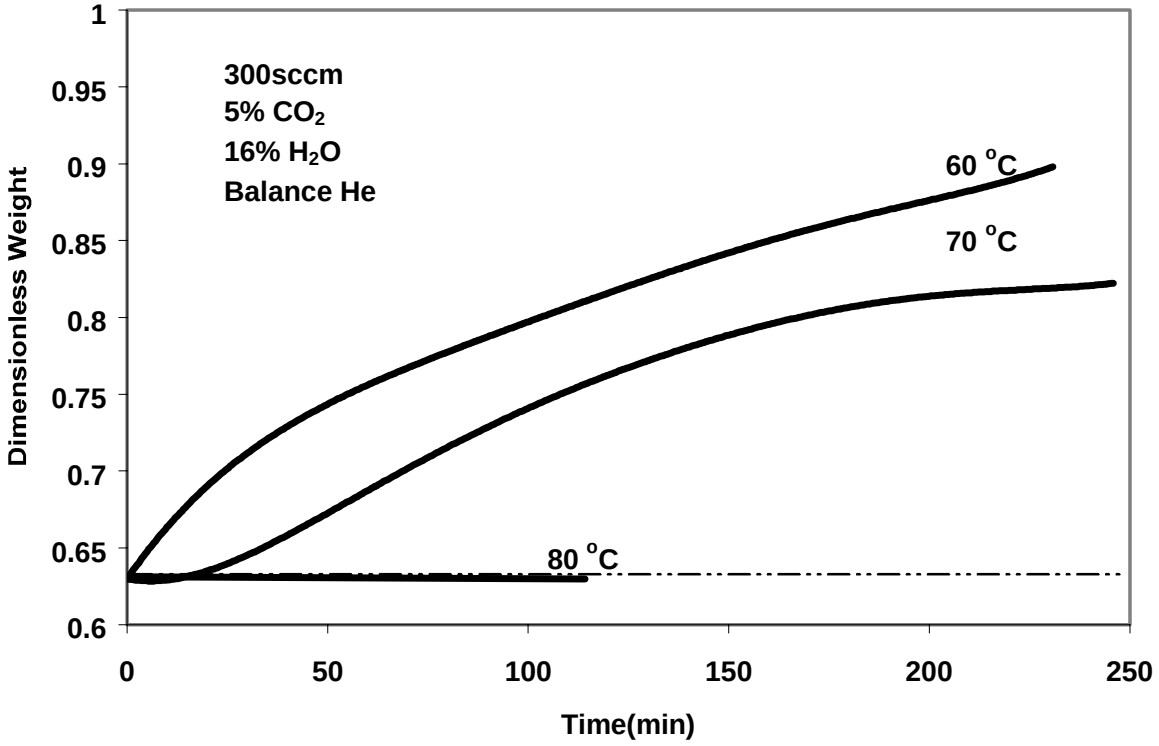

Figure 3. Effect of temperature in a carbonation gas containing 5% CO_2 and 16% H_2O

Figure 4 shows that reaction occurred at both 70°C and 80°C in an atmosphere containing 10% H_2O and 8% CO_2. The minimum CO_2 content required for $NaHCO_3$ formation in 10% H_2O predicted by HSC is 1.1% at 70°C and 4.1% at 80°C, so that the experimental results are consistent with thermodynamics. According to Table 2, no $NaCO_3 \cdot NaHCO_3 \bullet 2H_2O$ can be formed at either temperature, but $NaCO_3 \bullet 3NaHCO_3$ formation is possible at both the temperatures.

4.1.4 The Effect of CO_2 and H_2O Concentration

Increasing the CO_2 concentration at constant temperature and H_2O concentration produced a measurable increase in the reaction rate as shown in Figure 5. The sorbent capacity after 250 minutes was also greater in 8% CO_2 although extrapolation of the dimensionless weight versus time curves suggests that the ultimate achievable capacity for the two runs would be approximately equal.

Increasing the H_2O concentration at constant temperature and CO_2 concentration also produced an increase in the reaction rate as shown in Figure 6. However, the final achievable capacity was approximately the same at both H_2O concentrations. Note that these experimental results are counter to the preliminary RTI modeling analysis reported in the previous quarterly report (Green et al., 2001b) based upon the limited experimental results of Sarapata et al. (1987). That modeling study concluded that the rate was independent of both the CO_2 and H_2O concentrations and depended only on the extent of reaction.

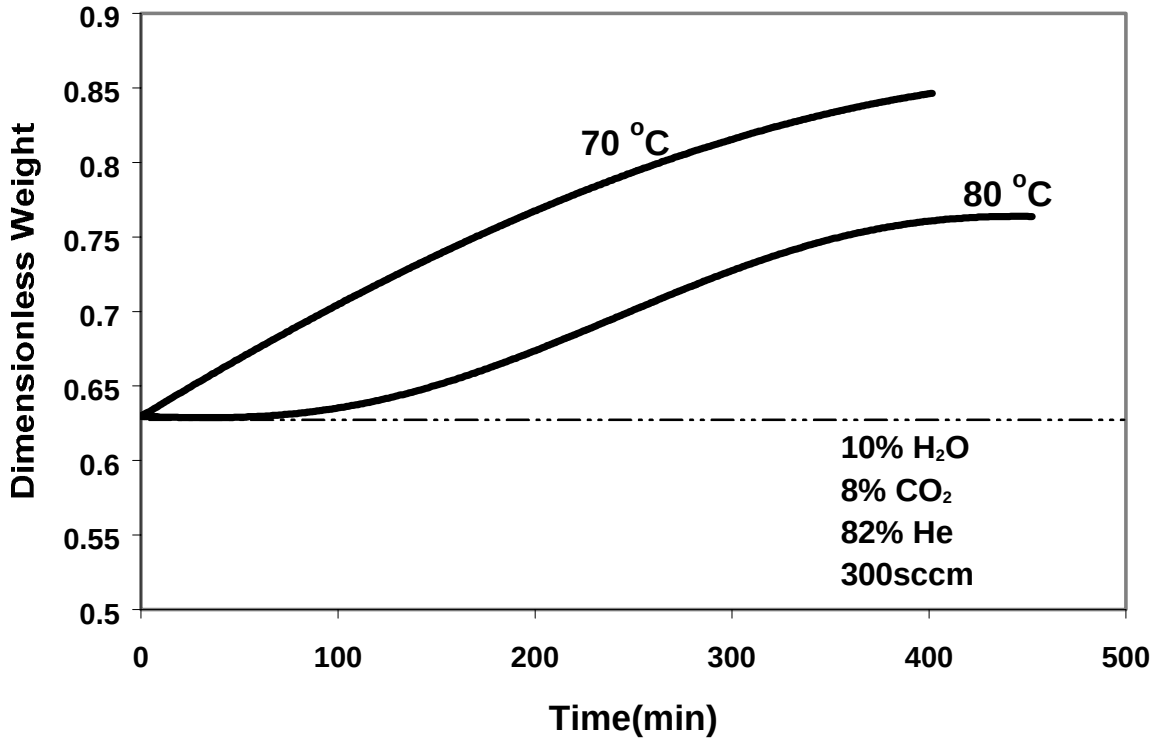

Figure 4. The effect of temperature in a carbonation gas containing 8% CO_2 and 10% H_2O

4.1.5 The Effect of Sample Pan and Initial Solid Weight

In all tests prior to run 31, the sorbent was contained in a quartz pan having the general shape of a cup so that only the top layer of sorbent was directly exposed to the reacting gas. Two tests (31 and 32) were made using an aluminum sample pan having a flatter shape thereby exposing more of the sample directly to the gas. In addition, in one of the tests (32) using the aluminum pan the initial sorbent charge was reduced to 30 mg from the standard charge of about 75 mg. Resulting dimensionless weight versus time curves at reaction conditions of 70°C in 5% CO_2 and 16% H_2O are compared in Figure 7.

The initial reaction rate was appreciably higher using the aluminum sample pan and the smaller initial charge, presumably because of improved initial gas-solid contact. However, after a relatively short time there was little difference in the results from the two types of sample pans. In spite of the slightly higher initial rate associated with the smaller initial sample charge, the rate decreased rapidly and the dimensionless weights from the tests using the larger samples were greater after about 75 minutes.

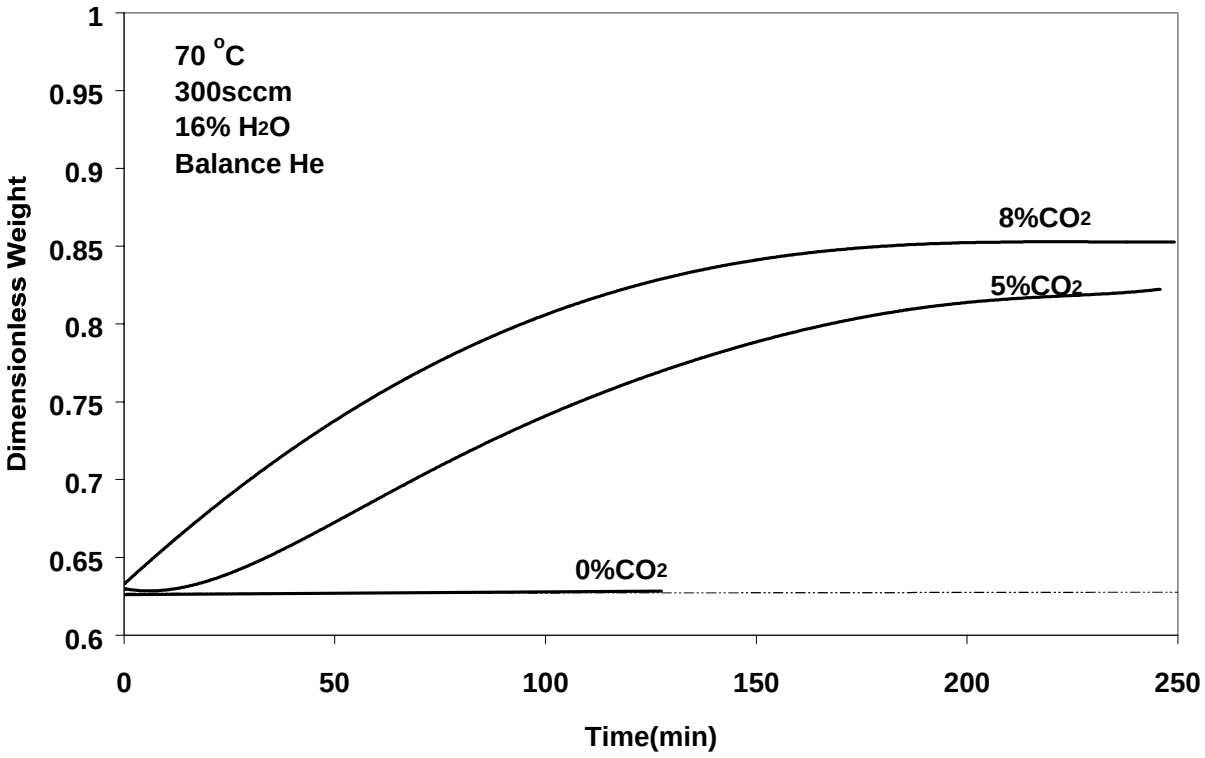

Figure 5. Effect of CO_2 concentration on reaction rate

4.1.6 The Effect of Volumetric Flow Rate

When the gas volumetric flow rate is small, the gas-to-solid mass transfer resistance may affect the global reaction rate. The standard volumetric feed rate of 300 sccm was chosen arbitrarily and additional tests using 600 sccm and 900 sccm were carried out. These tests used carbonation gas containing 8% CO_2 and 16% H_2O and the intended reaction temperature was 70°C. Precise control of reaction temperature proved to be difficult when the flow rate was varied because of the interplay between the manually controlled preheater and automatically controlled electrobalance heater. Sufficient preheat must be supplied to insure complete vaporization of the H_2O and to permit the electrobalance heater to boost the temperature to the desired reaction temperature. However, with too much preheat the temperature of the gas will exceed the intended reaction temperature. The proper level of preheat at a fixed feed rate can be determined only by trial and error. However, in these limited tests it was not possible to provide precise temperature control.

Dimensionless weight versus time results from four runs having a nominal reaction temperature of 70°C are shown in Figure 8. However, the actual temperature varied between 67°C and 73°C, which, as shown by previous results, can be quite significant. There is an appreciable increase in the global rate in the 600 sccm, 67°C run compared to the 300 sccm, 70°C run. The increased rate, however, may be due to either, or a combination of, the increased volumetric flow rate or the decreased reaction temperature. Results from the 900 sccm and 71°C run are very similar to results at 600 sccm and 67°C. In this case, however, the increased flow rate and temperature have opposing effects on the global rate. The negative

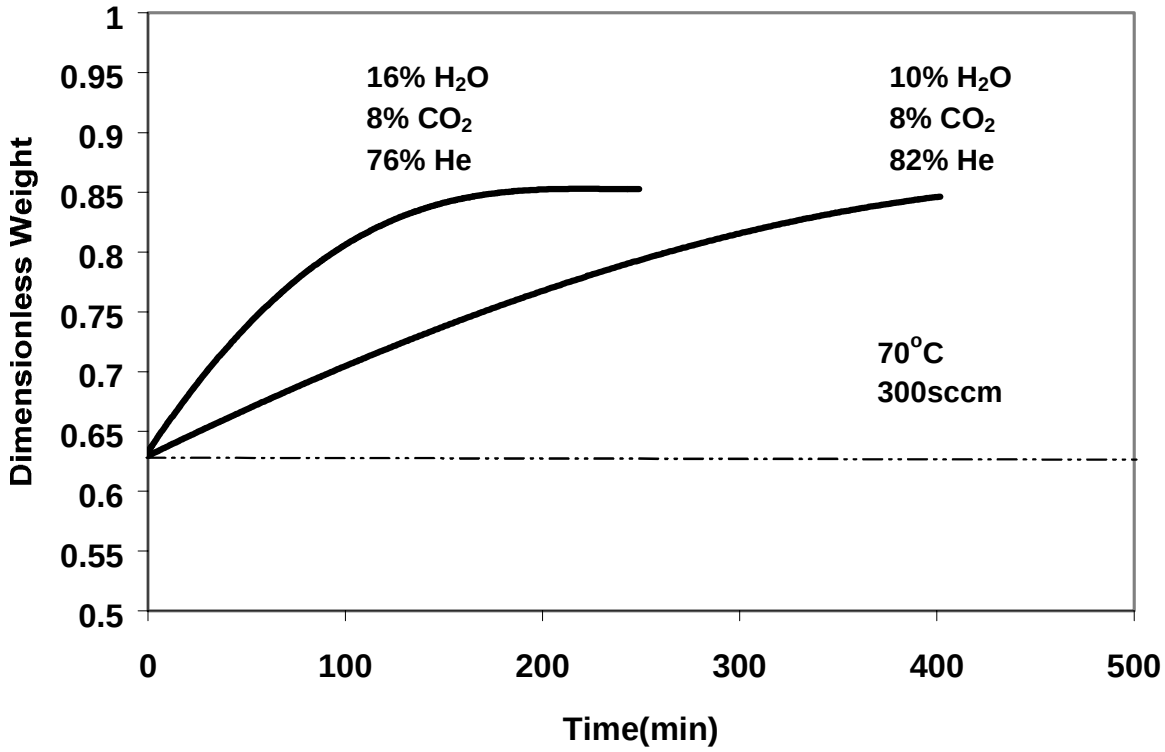

Figure 6. Effect of H_2O concentration on reaction rate

effect of increased temperature on global rate is seen by comparing results from the two runs at 600 sccm, one at 67°C and the other at 73°C. The higher temperature caused both the initial reaction rate and the achievable sorbent capacity to decrease, which is consistent with the effect of temperature at 300 sccm.

4.2 Fluidization Test Data

Fluidization tests were conducted on dried-in-place SBC 5 and calcined SBC 5 in the cold-flow test apparatus to obtain pressure drops and minimum fluidization velocities for design of the fluidized-bed reactor system. Both materials were tested at 22°C with sorbent masses of 2.5 kg. Test results are presented in Figures 9 and 10.

Both the dried SBC grade 5 and the sodium carbonate material calcined from SBC grade 5 were completely fluidized at pressure drops of approximately 11 inches of water which compounds to a minium fluidization velocity of about 7 ft/min.

4.3 Material Testing at RTI

Repeat determinations of the BET surface area of SBC 5 were conducted. The fresh material was found to have a surface area of 4.1 m^2/g, in contrast to the earlier determination of 5.9 m^2/g.

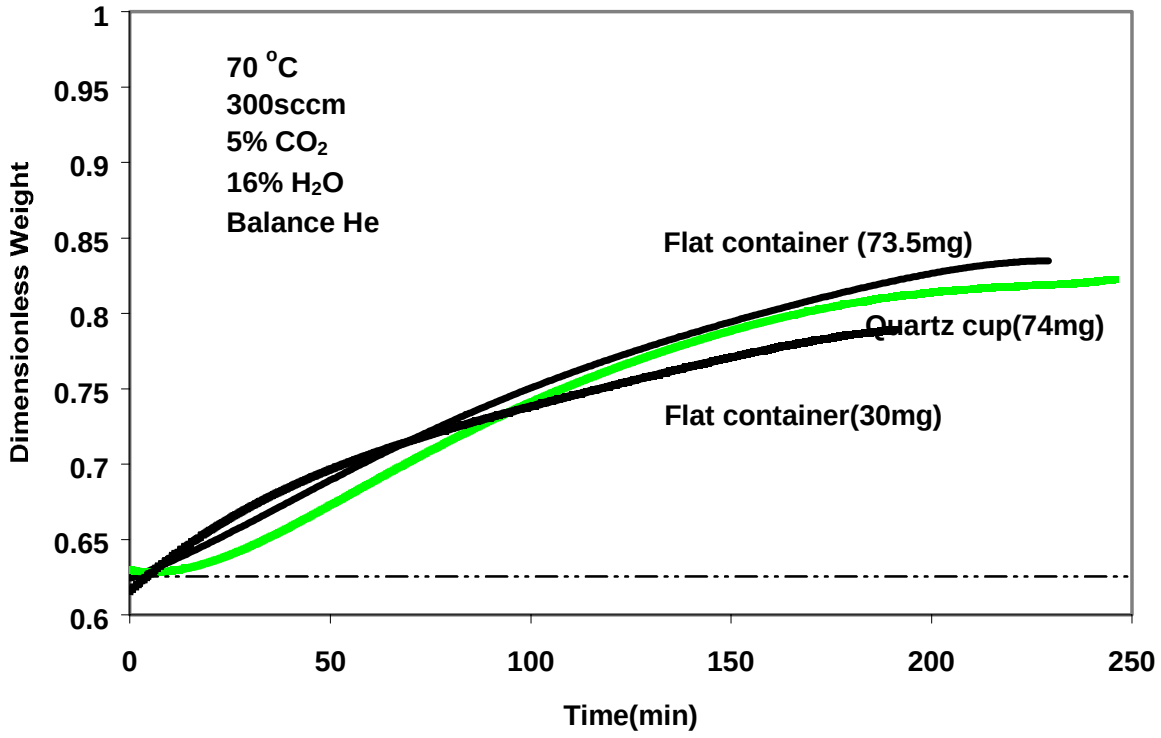

Figure 7. Effect of pan shape and initial sorbent charge

The calcined material was determined to have a BET surface area of 2.2 m^2/g, in contrast to 2.5 m^2/g which was reported in the first quarterly report.

Bulk density determinations were also conducted. Fresh SBC 5 and calcined SBC 5 had bulk densities of 69.7 and 43.8 lb/ft^3, respectively.

4.4 Kinetic Analysis

In the past quarter RTI has begun an effort to analyze kinetic data from the LSU electrobalance work. This effort has been directed towards developing kinetic models of the data for application to other types of reactors. Specific models for reactors such as fast fluidized had reactors can be used to predict the performance of these systems.

Much of the work has been based on Figure 4 of the previous quarterly report (Green et al., 2000b), reproduced below, as Figure 11.

These data were obtained in the LSU TGA by reacting fully calcined sodium bicarbonate in an atmosphere of 8 percent CO_2, 16 percent H_2O, balance helium, at temperatures of 60°C, 70°C, and 80°C. An interesting aspect of these data is that the apparent initial reaction rates of sodium carbonate to sodium bicarbonate appear to counterintuitively decrease with increasing reaction temperature. The reason for this, as explained in the previous quarterly report, is that as the temperature is increased, there exists an increasingly higher back pressure of reactants

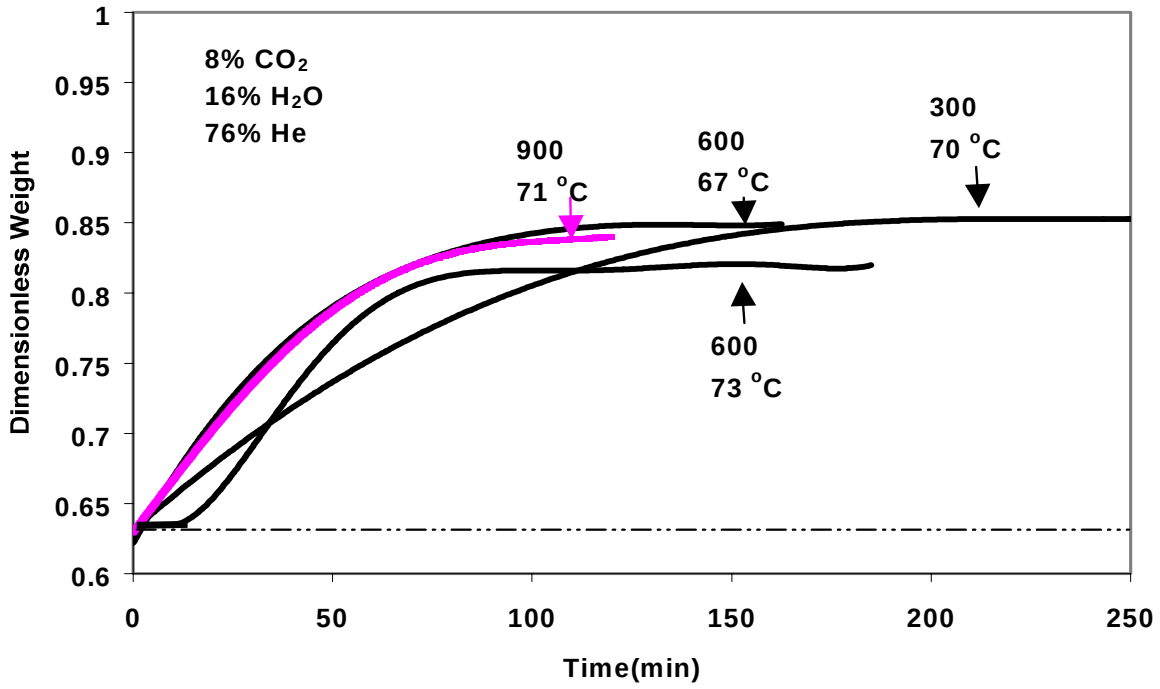

Figure 8. Effect of volumetric flow rate on reaction rate

which reduces the overall driving potential of the reactants to diffuse to the surface of the sodium carbonate.

Assuming that at a given temperature, the diffusion potential remains practically constant with time over the duration of the run, and further assuming that the reaction rate is proportional to the amount of sodium carbonate left in the sample in the TGA pan, the following reaction rate expression can be derived:

$$\frac{dx}{dt} = k(1 - X) \qquad (5)$$

where X = the conversion of sodium carbonate to sodium bicarbonate, dimensionless
k = apparent reaction rate constant which includes diffusional potential, min^{-1}
and t = time, min.

For the initial conditions, x=0 at t=0, Equation (5) integrates to:

$$-\ln(1 - X) = kt \; . \qquad (6)$$

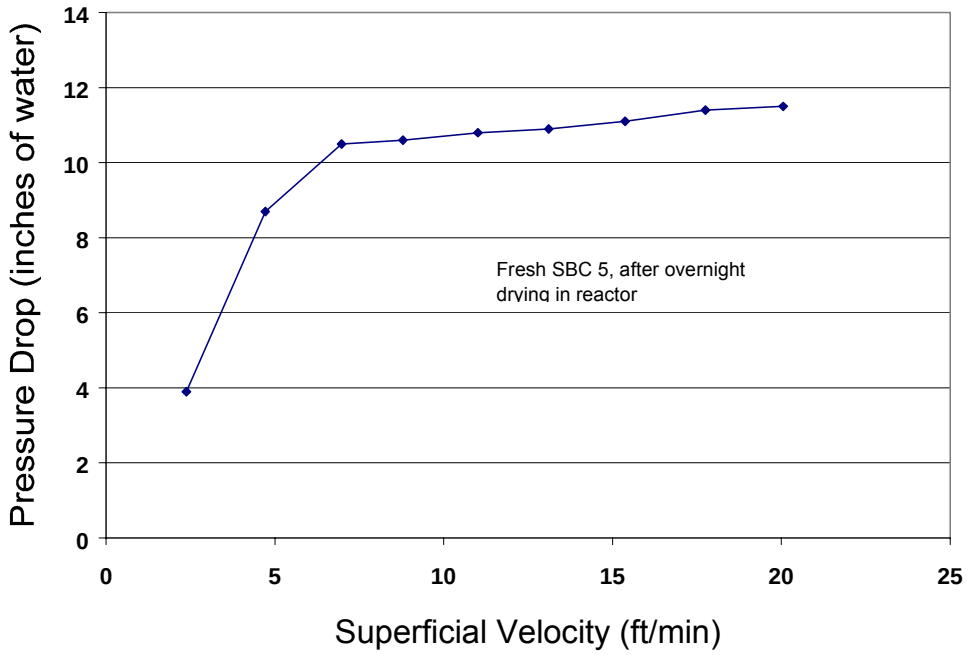

Figure 9. Fluidization of dried SBC grade 5

As can be seen from Equation (6), the proportionality constant, k, represents the initial reaction rate (i.e. X=0). Plotting the data shown in Figure 11, in the form suggested by Equation (6) yields Figure 12. As can be seen in this figure, Equation (6) fits the data reasonably, even at fairly high conversions. Thus, if the initial rate of reaction could be determined, this initial rate, k, may be useful in predicting reaction rates at higher conversions.

At the initiation of the reaction of CO_2 and H_2O with Na_2CO_3 to form $NaHCO_3$, it might be expected that the rate of reaction is controlled by transfer of mass and heat to the external surface of the Na_2CO_3 particle and gas/solid chemical reaction rate at the particle surface. Thus the rate of CO_2 transfer to the surface of the particle from the bulk gas phase is given by,

$$n_{CO_2} = k_{gCO_2}(P_{CO_2} - P^{S}_{CO_2}) \tag{7}$$

and the rate of H_2O transfer is given by,

$$n_{H_2O} = K_{gH_2O}(P_{H_2O} - P^{S}_{H_2O}) \tag{8}$$

where n_{CO2} = the flux of CO_2 to the surface of the particle, gmol CO_2/(cm^2 sec),

n_{H2O} = the flux of H_2O to the surface of the particle, gmol H_2O/(cm^2 sec),

k_{gCO2} = the mass transfer coefficient for CO_2, gmol/(atm cm^2 sec),

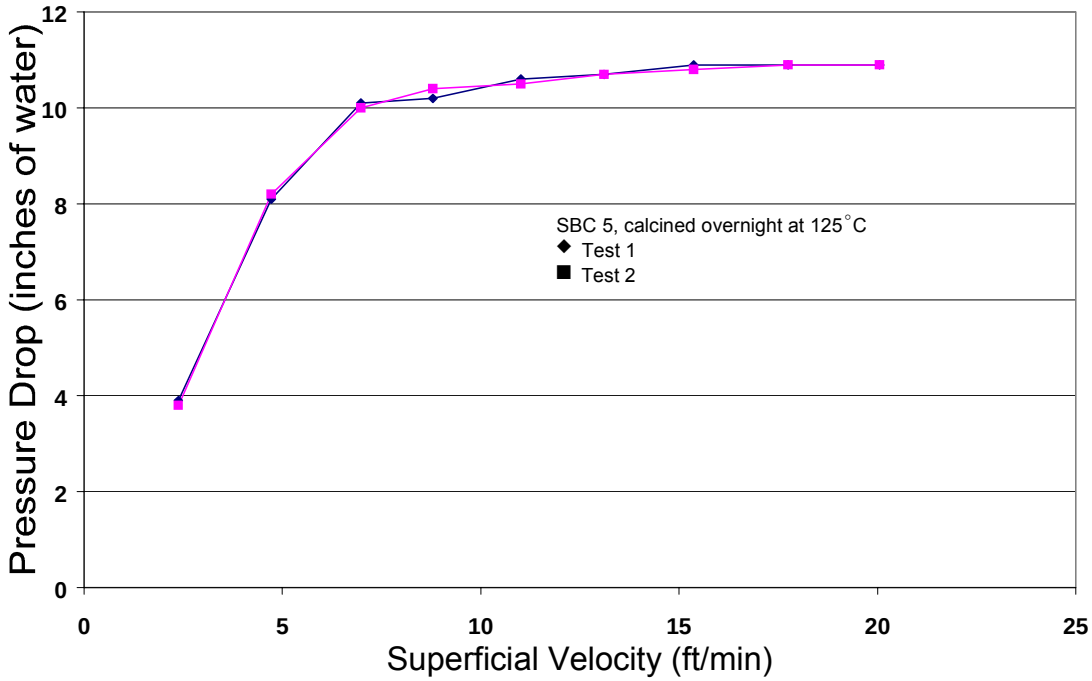

Figure 10. Fluidization of calcined SBC grade 5

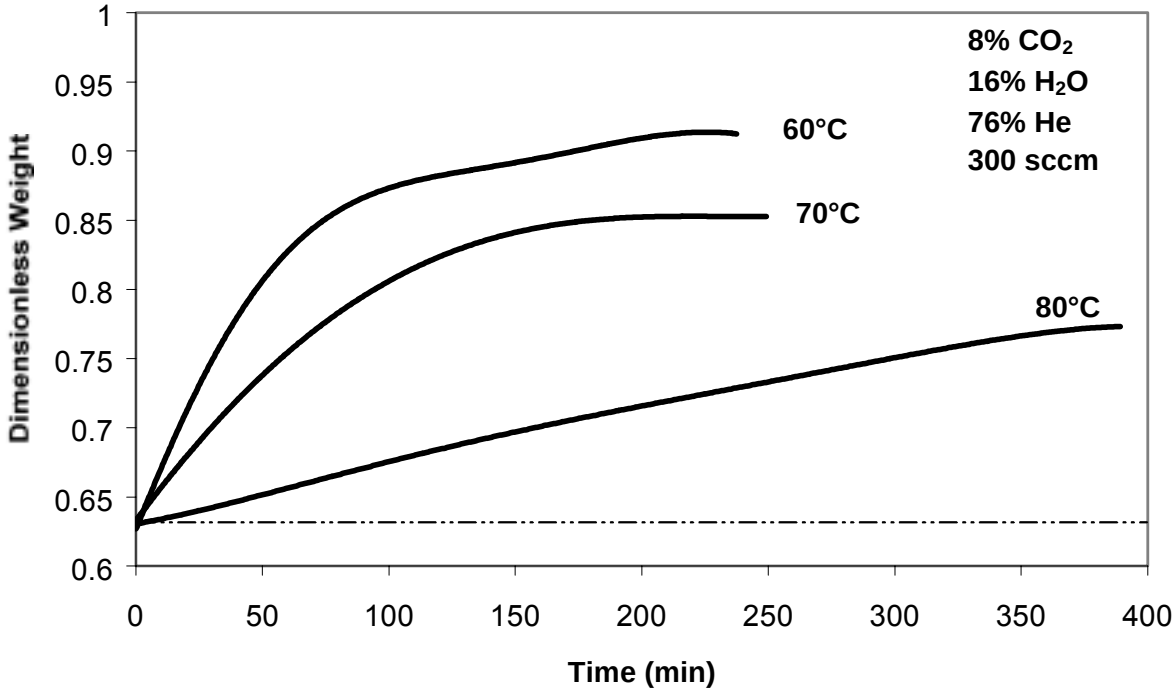

Figure 11. Effect of carbonation temperature using SBC grade #3

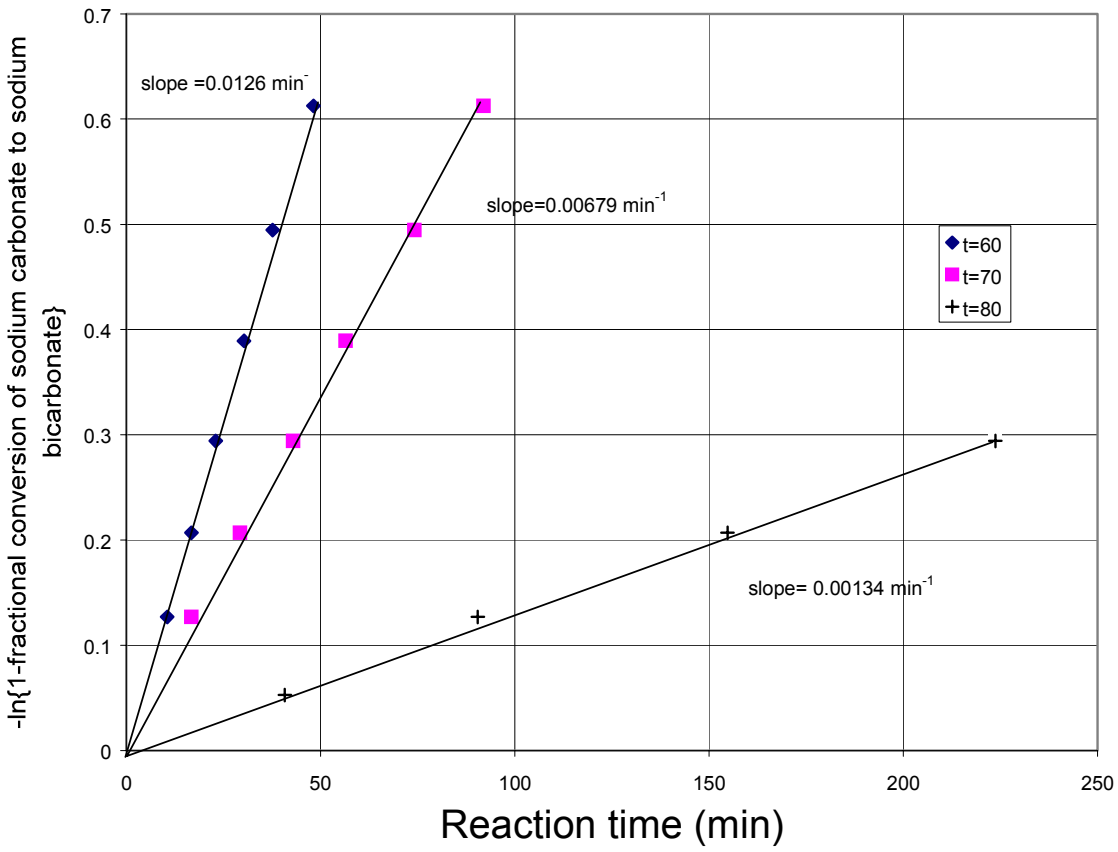

Figure 12. Plot of data of Figure 11

k_{gH2O} = the mass transfer coefficient for H_2O, gmol/(atm cm^2 sec),

P_{CO2} = the partial pressure of CO_2 in the bulk gas phase, atm,

P_{H2O} = the partial pressure of H_2O in the bulk gas phase, atm,

P^s_{CO2} = the partial pressure of CO_2 at the surface of the Na_2CO_3 particle, atm,

and, P^s_{H2O}= the partial pressure of H_2O at the surface of the Na_2CO_3 particle, atm.

If it is further assumed that the reaction,

$$Na_2CO_3 + H_2O + CO_2 \rightarrow 2NaHCO_3 \qquad (9)$$

is at equilibrium at the particle surface, then,

$$P^sCO_2 P^sH_2O = K^{-1} \qquad (10)$$

where K = the equilibrium constant, atm^{-2}.

Setting the fluxes of CO_2 and H_2O equal, $n_{CO2} = n_{H2O}$, and using the equilibrium condition (Equation 10), the partial pressure of carbon dioxide at the surface of the particle is:

$$P^{S}_{CO_2} = \frac{-(\alpha P_{H_2O} - P_{CO_2}) + \sqrt{(\alpha P_{H_2O} - P_{CO_2})^2 + 4\alpha K^{-1}}}{2} \qquad (11)$$

where $\alpha = \frac{k_{gH_2O}}{k_{gCO_2}}$.

For the gas composition used in the experiment plotted in Figure 11, at 70°C,

$$\alpha \approx \frac{D_{H_2O}}{D_{CO_2}} = 2.38.$$

Applying Equation 11 to the conditions of the three runs shown in Figure 11 yields the data shown in Table 3.

Table 3. Rate Constants for Figure 11 (8 % CO_2 and 16%H_2O)

Gas Temperature	K^{-1}	P^s_{CO2}	P_{CO2}-P^s_{CO2}	k (from Fig. 12)	k'
°C	atm^2	atm	atm	min-1	$(min\ atm)^{-1}$
60	0.00213	0.0160	0.0640	0.01260	0.197
70	0.00824	0.0551	0.0249	0.00679	0.270
80	0.02949	0.2309	negligible	SBC will not form	n/a

As indicated in Table 3, sodium bicarbonate will not form at 80°C, and the weight gain at 80°C as shown in Figure 11, is most likely due to the formation of $Na_2CO_3 \bullet 3NaHCO_3$. The last column of Table 3, indicates the quantity k', which is the proportionality constant between the initial reaction rate, k, and the partial pressure driving potential, P_{CO2}-P^s_{CO2}. Thus,

$$k = k'(P_{CO_2} - P^{S}_{CO_2}) \qquad (12)$$

As can be seen from Table 3, k' increases with increased temperature. Based on two temperatures of 60°C and 70°C,

$$k' = k'_0 \, \ell^{-3727/T} \tag{13}$$

where T is in degree Kelvin. Thus the activation energy of 3727 times R, or 7405 cal/gmol is considered high for a diffusional process. This point will be investigated in the future using the TGA data developed by LSU that has been reported this quarter.

In the calculation of the partial pressure of carbon dioxide at the solid surface carried out above and summarized in Table 3, it was assumed that the surface of the sodium carbonate particle had the same temperature as the bulk gas. Because the reaction of sodium carbonate with carbon dioxide and water to form sodium bicarbonate is highly exothermic (about 30.69 kcal/gmol of sodium carbonate), the surfaces at which the reaction is occurring can be at a much higher temperature than their surroundings. Smith (1970) has described in detail the situation of an exothermic chemical reaction occurring at a surface to which reactants are diffusing. Smith found that for a reacting particle in a packed bed, the temperature of the surface with respect to the bulk gas temperature is given by,

$$T_s - T \approx \frac{0.7(-\Delta H_R)}{C_p \rho}(C - C_s) \tag{14}$$

where T_s = temperature of the solid surface, K
T = temperature of the bulk gas, K
ΔH_R = enthalpy of reaction, cal/gmol of gaseous reactant
Cp = heat capacity of the gas, cal/(gmol°K)
ρ = density of gas, gmol/cm^3
C = concentration of the diffusing gas, gmol/cm^3,
and C_s = concentration of the diffusing gas at the solid surface, gmol/cm^3.

Equation 14 results from balancing the rate at which heat is generated at the surface of the solid particle by diffusion of the reactant to the solid surface and subsequent reaction and heat release, with the rate at which heat is transferred away from the surface to the bulk gas.

For the case shown in Figure 11, at 60°C and total pressure P_T of 1 atm,

$$\frac{C - C_s}{\rho} = \frac{P_{CO_2} - P^s_{CO_2}}{P_T} \approx 0.0640 \tag{15}$$

Substituting this into Equation (14), and noting that (ΔH_R) = 30,690 cal/gmol, yields:

$$T_s - T = (0.7)(30690)(0.064) / 7 = 196 \text{ K} \tag{16}$$

Thus if the bulk gas temperature is 60°C, the surface of the sodium carbonate particle will be approximately 60+196 =256°C. But, at a gas composition of 0.08 atm carbon dioxide and 0.16 atm water, the reaction of sodium carbonate to sodium bicarbonate will not proceed at temperatures above 73.4°C.

In Equation 11, the partial pressure of carbon dioxide at the solid surface, P^s_{CO2}, is a function of the surface temperature through the equilibrium constant, K. Thus Equations 11, 14 and 15 could be solved for P^s_{CO2} and T_s. Thus, once either one of these quantities is known, knowledge of heat or mass transfer correlations would allow the initial rate of reaction, k (at X=0), of sodium carbonate to sodium bicarbonate to be calculated. This initial rate could then be extrapolated to higher conversion using equation (6).

Solving Equations 11, 14 and 15 for P^s_{CO2} and T_s depends on the environment on the reacting particle. Equation (11) was derived (Smith, 1970) for a particle in a packed bed. Similar calculations could be derived for fluidized beds and TGA baskets. In each of these cases, because of the high heat of reaction, a small difference in the partial pressure of carbon dioxide in the bulk gas with respect to the solid surface will make a large change in the solid surface with respect to the bulk gas temperature. Therefore the approximate solution of Equations 14 and 15, and a system-specific equation such as Equation (11), will be $T_s = T_{eq}$, where T_{eq} satisfies,

$$K(T_{eq}) = (P_{CO_2} P_{H_2O})^{-1}. \tag{17}$$

The actual value of the surface temperature, T_s will be slightly less than T_{eq}, the equilibrium temperature. Thus, unless the bulk gas temperature, T, is near the equilibrium temperature, T_{eq}, as determined by the bulk gas composition, the driving force for heat removal from the surface of the carbonate particle, T_s - T, can be approximated by T_{eq} -T. Thus,

$$[\text{Reaction rate}] = N^o_{Na2CO3} \frac{dX}{dt} = \frac{hA(T_{eq} - T)}{-\Delta H_R} \tag{18}$$

where N^o_{Na2CO3} = initial moles of Na_2CO_3 in the particle at t=0, gmol,

h = the heat transfer coefficient, cal/(cm^2 K sec),

and A = the area of the particle, cm^2.

Equation (18) shows that the initial reaction rate for the reaction of sodium carbonate to sodium bicarbonate may be directly calculable from heat transfer data.

To test this concept, Equation (18) can be rearranged to give:

$$\text{Rate}_{initial} = k = \left.\frac{dX}{dt}\right|_{t=0} = h'(T_{eq} - T_b) \tag{19}$$

where $h' = \dfrac{hA}{N_{Na2CO3}(-\Delta H_R)}$.

Thus, for any given particle geometry, the proportionality constant, h', should be a weak function of temperature. To test this, the TGA data shown in Figure 11, and the fluidized bed data of Sarapata et al. (1987) have been used to calculate h' for each of the data points. The data of Sarapata et al. were taken from a batch fluidized bed reactor to which an initial amount

of sodium carbonate and sodium bicarbonate was added. After passing a mixture of steam, carbon dioxide and nitrogen at 1 atm pressure and a specified temperature, the bed was emptied once or twice, and the amount of sodium carbonate remaining was determined. The initial reaction rate, k, was not determined, however k was estimated using Equation (6) at high sodium carbonate conversions.

The calculation of the heat transfer proportionality constant, h', using Equation (19), is shown stepwise in Table 4. The results obtained in Table 4, are summarized in Figure 13, where the heat transfer proportionality constant is shown as a function of bed temperature in the case of the data of Sarapata et. al., and as a function of bulk gas temperature for the data of Green et al., 2001b.

As shown in Figure 12, h' is a strong function of temperature with an activation energy of 13.1 kcal/gmol. Prior to carrying out the calculations shown in Table 4, it was anticipated that h' would be a weak function of temperature. The fact that both the data of Sarapata et al. and Green et al. give approximately the same activation energy may point to a systematic error in the calculations.

The approach of estimating initial reaction rate and then extrapolating that rate to higher conversion has the advantage of simplicity and can use available heat and mass transfer correlations for various reactor configurations to estimate reaction rates. The real kinetic mechanism is more complex in that,

1) more than one solid species can be formed in a single particle of sodium carbonate, depending on local temperatures and gas compositions within the particle; and
2) temperature and composition fronts can move through the particle.

More work is needed in formulating a mechanism of reaction and in formulating the mathematics describing that mechanism. During the past quarter, many TGA experiments have been performed; these results are included in this report, and should form a solid basis for extending the kinetic interpretation work described above and for developing a more comprehensive kinetic model of the reaction of sodium carbonate with carbon dioxide and water.

4.5 Process Simulation

Simulation work continued at RTI focusing on balancing the heat effects in a cyclic carbonation/calcination process. Figure 14 is a schematic of a process based on flue gas available at a temperature of 250°C. This process captures approximately 26 percent of the carbon dioxide present from a flue gas stream with an initial carbon dioxide concentration of 11.6 percent. Mass and energy balances for the numbered streams in the schematic are given in Table 5.

4.6 Plans for Next Quarter

In the next quarter LSU will continue electrobalance tests of sodium based sorbents to study the effects of temperature, gas composition, and gas volumetric flow rate using a number of candidate sorbent materials. Multicycle tests will be conducted to study sorbent durability. RTI will extend kinetic modeling studies based on data obtained by LSU in the present quarter, and

Table 4. Summary of Results from Applying Equation 19 to the Data of Sarapata et al. (1987) and Green et al. (2001b).

Example*	Temp	Inlet Gas		Equil.		Reaction			
		P_{CO2}	P_{H2O}	Temp.	T_{eq}-T	X_{Na2CO3}	time, t	k, (Eq 6)	h' (Eq 19)
	(°C)	(atm)	(atm)	(°C)	(°C)		(min)	(min^{-1})	$(min\ °K)^{-1}$
II	90	0.300	0.700	96	6	0.8085	20	8.26×10^{-2}	1.38×10^{-2}
III	70	0.135	0.307	83	13	0.9113	45	5.38×10^{-2}	4.14×10^{-3}
IV	50	0.107	0.123	74	24	0.6614	40	2.71×10^{-2}	1.13×10^{-3}
IV	50	0.107	0.123	74	24	0.9117	50	4.85×10^{-2}	2.02×10^{-3}
V	50	0.062	0.123	69	19	0.8744	70	2.96×10^{-2}	1.56×10^{-3}
VI	31	0.113	0.0459	66	35	0.8645	260	7.69×10^{-3}	2.20×10^{-4}
VII	31	0.143	0.0459	68	37	0.8362	160	1.13×10^{-2}	3.05×10^{-4}
VII	31	0.143	0.0459	68	37	0.9230	180	1.42×10^{-2}	3.84×10^{-4}
TGA (60°)	60	0.08	0.16	74	14			1.26×10^{-2}	9.00×10^{-4}
TGA (70°)	70	0.08	0.16	74	4			6.79×10^{-3}	1.70×10^{-3}

*Example numbers are based on Sarapata (1987).

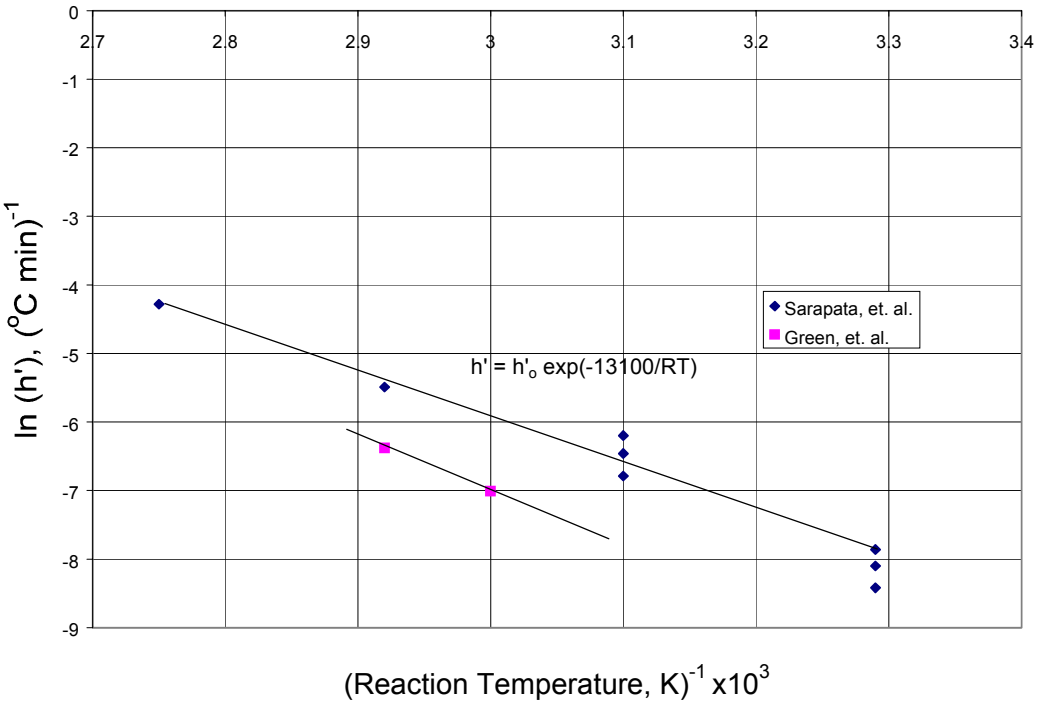

Figure 13. Effect of bed or bulk gas temperature on heat transfer proportionality constant, h'.

develop a design for a fluidized bed reactor system. Preliminary testing on other materials including sodium carbonate monohydrate will be conducted.

5.0 CONCLUSIONS

1. Additional data collected during the quarter confirmed that the reaction rate and achievable CO_2 capacity decreased with increasing temperature using $NaHCO_3$ sorbent precursor.

2. Experimental data showed that $Na_2CO3•H_2O$ is formed at carbonation conditions of potential interest, and thermodynamic analysis indicated the possible formation of $Na_2CO_3•NaHCO_3•2H_2O$ and $Na_2Co_3•3NaHCO_3$ at conditions of interest. Electrobalance data cannot distinguish contributions from individual reactions when simultaneous gas-solid reactions occur.

3. At constant temperature, the global reaction rate increases with an increase in both CO_2 and H_2O concentrations, in contrast to preliminary modeling analysis that showed the rate to be a function only of extent of solid reaction.

4. The shape of the sample pan, quartz cup versus flat aluminum plate, had relatively little effect on the global rate.

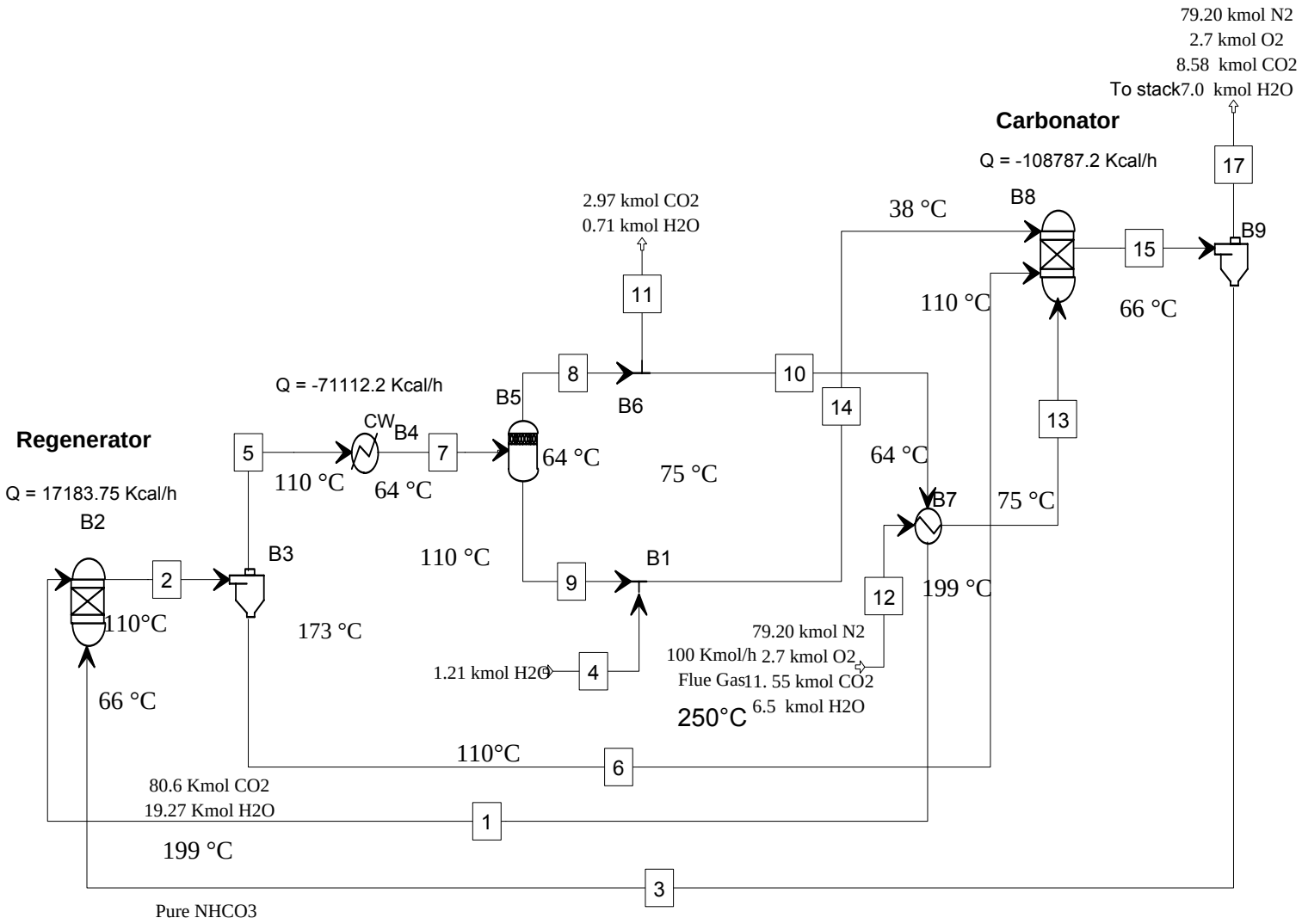

Figure 14. Schematic of cyclic carbon dioxide capture process based on 250 C flue gas

Table 5. Process Material and Energy Balances

Stream ID	1	2	3	4	5	6	7	8	9	10	11	12	13	14	15	17
Temperature (C)	199	110		63.4	110		63.4	63.4	63.4	63.4	63.4	250	75	38.2	66	66
Pressure (bar)	1	1		1	1		1	1	1	1	1	1	1	1	1	1
Vapor Frac	1	1		0	1		0.979	1	0	1	1	1	1	0	1	1
Mole Flow (kmol/hr)	99.9	105.8	0.0	1.2	105.8	0.0	105.8	103.6	2.3	99.9	3.7	100.0	100.0	3.5	97.5	97.5
Mass Flow (kg/hr)	3895.6	4079.8	0.0	21.8	4079.8	0.0	4079.8	4039.1	40.7	3895.6	143.5	2930.5	2930.5	62.5	2808.8	2808.8
Volume Flow (cum/hr)	3917.2	3371.7	0.0	1.2	3371.7	0.0	2885.5	2885.5	0.0	2782.9	102.5	4348.8	2892.3	3.5	2748.8	2748.8
Enthalpy (kcal/mol)	-85.4	-85.6		-67.5	-85.6		-86.3	-86.7	-68.2	-86.7	-86.7	-12.9	-14.3	-68.0	-12.1	-12.1
Mole Flow (kmol/hr)																
N_2												79.2	79.2		79.2	79.2
O_2												2.7	2.7		2.7	2.7
CO_2	80.6	83.6			83.6		83.6	83.6	< 0.001	80.6	3.0	11.6	11.6	< 0.001	8.6	8.6
H_2O	19.3	22.2		1.2	22.2		22.2	20.0	2.3	19.3	0.7	6.5	6.5	3.5	7.0	7.0
NA2CO3																
NAHCO3																
Mass Flow (kg/hr)	3895.61	4644.12	748.502	21.798	4079.84	564.287	4079.84	4039.12	40.72	3895.61	143.503	2930.48	2930.48	62.519	3557.28	2808.78
Enthalpy MMkcal/hr	-8.527	-10.522	-2.012	-0.082	-9.06	-1.462	-9.131	-8.977	-0.154	-8.658	-0.319	-1.294	-1.425	-0.236	-3.193	-1.182
SOLID PHASE																
Temperature (C)		110	66			110									66	
Pressure bar	1	1	1	1		1	1	1	1	1	1	1	1	1	1	
Vapor Frac		0	0			0									0	
Mole Flow (kmol/hr)	0	5.94	8.91	0	0	5.94	0	0	0	0	0	0	0	0	8.91	0
Mass Flow (kg/hr)	0	564.287	748.502	0	0	564.287	0	0	0	0	0	0	0	0	748.502	0
Volume Flow (cum/hr)	0	0.237	0.338	0	0	0.237	0	0	0	0	0	0	0	0	0.338	0
Enthalpy (kcal/mol)		-246.05	-225.77			-246.05									-225.77	
Mole Flow (kmol/hr)																
N_2																
O_2																
CO_2																
H_2O																
NA2CO3		2.97				2.97										
NAHCO3		2.97	8.91			2.97									8.91	

5. Inconclusive data suggest that the reaction rate at the standard volumetric feed rate of 300 sccm may be somewhat limited by mass transfer resistance. The data are inconclusive because carbonation temperature could not be adequately controlled at higher feed rates.

6. The rate of heat removal from the particle surface may determine the reaction rate for a particular reactor system. Because the reaction of sodium carbonate with carbon dioxide and water is highly exothermic, the surfaces at which the reaction is occurring can be at a much higher temperature than the bulk gas.

7. Based on reaction rate data obtained during the preceding quarter, the reaction of sodium carbonate with carbon dioxide and water has an activation energy of approximately 7,405 cal/gmol, which is high for a diffusional process.

6.0 REFERENCES

Green, D.A., Turk, B.S., Gupta, R., and Lopez Ortiz, A., Carbon Dioxide Capture From Flue Gas Using Dry Regenerable Sorbents, Quarterly Technical Progress Report, Research Triangle Institute, January 2001(a).

Green, D.A., Turk, B.S., Gupta, R., and Lopez Ortiz, A., Harrison, D. P., and Liang, Y., Carbon Dioxide Capture From Flue Gas Using Dry Regenerable Sorbents, Quarterly Technical Progress Report, Research Triangle Institute, May 2001(b).

Sarapata, J.S., et al., “Method for the Preparation of a Bicarbonate Sorbent in Flue Gas Desulfurization.” U.S. Patent No.: 4,664,893, assigned to C & D. May 12, 1987.

Smith, J. M., "Chemical Engineering Kinetics", McGraw-Hill Book Company, New York, 1970.